

Nicotinamide Mononucleotide Adenylyltransferase 1 Regulates Cerebral Ischemia-Induced Blood–Brain Barrier Disruption Through NAD⁺/SIRT1 Signaling Pathway

Yang Zhang

Jinzhou Medical University

Xun Guo

Jinzhou Medical University

Zhifeng Peng

Shanxi Datong University

Chang Liu

Jinzhou Medical University

Lili Ren

Jinzhou Medical University

Jia Liang

Jinzhou Medical University

Peng Wang (✉ wangpeng@jzmu.edu.cn)

Jinzhou Medical University <https://orcid.org/0000-0001-9660-0147>

Research Article

Keywords: ischemic stroke, BBB, NMNAT1, NAD⁺, SIRT1

Posted Date: November 16th, 2021

DOI: <https://doi.org/10.21203/rs.3.rs-1049423/v2>

License: © ⓘ This work is licensed under a Creative Commons Attribution 4.0 International License.

[Read Full License](#)

Abstract

The molecular mechanisms of blood–brain barrier (BBB) disruption in the early stage after ischemic stroke are poorly understood. In the present study, we investigated the potential role of nicotinamide mononucleotide adenylyltransferase 1 (NMNAT1) in ischemia-induced BBB damage using an animal middle cerebral artery occlusion (MCAO) model of ischemic stroke. Recombinant human NMNAT1 (rh-NMNAT1) was administered intranasally and Sirtuin 1 (SIRT1) siRNA was administered by intracerebroventricular injection. Our results indicate that rh-NMNAT1 reduced infarct volume, improved functional outcome and decreased BBB permeability in mice after ischemic stroke. Furthermore, rh-NMNAT1 prevented the loss of tight junction proteins (occludin and claudin-5) and reduced cell apoptosis in ischemic microvessels. NMNAT1-mediated BBB permeability was correlated with the elevation of nicotinamide adenine dinucleotide (NAD⁺)/NADH ratio and SIRT1 level in brain microvascular endothelial cells. In addition, rh-NMNAT1 treatment significantly decreased the levels of acetylated nuclear factor- κ B, acetylated p53 and matrix metalloproteinase-9 in ischemic microvessels. Moreover, the protective effects of rh-NMNAT1 could be reversed by SIRT1 siRNA. In conclusion, these findings indicate that rh-NMNAT1 protects BBB integrity after cerebral ischemia via the NAD⁺/SIRT1 signaling pathway in brain microvascular endothelial cells. NMNAT1 may be a novel potential therapeutic target for reducing BBB disruption after ischemic stroke.

Introduction

Blood-brain barrier (BBB) damage in the early stage of ischemic stroke is closely associated with parenchymal cell injury and regarded as a vital therapeutic target for ischemic stroke [1, 2]. Thus, it is necessary to explore the mechanism of BBB permeability regulation. The matrix metalloproteinases (MMPs), especially MMP-9 (also known as gelatinase B), play a vital role in mediating BBB permeability after ischemic stroke [3, 4]. MMP-9 is increased during cerebral ischemia and leads to BBB breakdown via proteolytic degradation of endothelial tight junction proteins (TJPs) [5, 6]. Death of brain microvascular endothelial cells is also an important contributor to BBB disruption [7]. Therefore, both degradation of TJPs and death of brain microvascular endothelial cells should be considered to protect BBB integrity.

Nicotinamide mononucleotide adenylyltransferase 1 (NMNAT1), an essential enzyme in nicotinamide adenine dinucleotide (NAD⁺) synthesis, is considered as a potential therapeutic target for several diseases because of its vital role in NAD⁺ production in cells [8-10]. Recently, several evidences have implicated the vital roles of NMNAT1 in a broad range of pathological conditions. Mutation of NMNAT1 promotes retinal degeneration in a mouse model through the direct effect on NAD⁺ biosynthesis [11-13]. NMNAT1 substantially decreases multiple Alzheimer's disease-associated pathological characteristics partially by inhibiting caspase-3 signaling [14]. It has been reported that depletion of NAD⁺ that participates in many important intracellular signaling pathways is a common pathway in the development of pathophysiological status, including aging and cerebral ischemia [15-18]. Sirtuin 1 (SIRT1), the nuclear NAD⁺-dependent protein deacetylase, has been shown to regulate the activation of

MMP-9 during cerebral ischemia [19]. NAD⁺ positively regulates the expression of SIRT1 and NAD⁺/SIRT1 pathway plays protective roles in cerebral ischemia [19, 20]. Though NMNAT1 has been reported to play a critical role in cerebral ischemic injury in mammals [21, 22], but whether NMNAT1 exerts any effects on BBB integrity after cerebral ischemia remains unknown.

In the present study, our hypothesis is that intranasal administration of NMNAT1 could attenuate ischemic brain damage by maintaining BBB integrity and the underlying mechanism might involve NAD⁺/SIRT1 signaling pathway. This study could provide a novel therapeutic target for ischemic stroke.

Materials And Methods

Middle cerebral artery occlusion (MCAO)

Male C57BL/6 J mice (2-3 months old, 20-25 g) were maintained in temperature-controlled rooms with 12 h light/dark cycles where they received food and water ad libitum. A total of 238 male mice (Vital River Laboratory Animal, Co) were used in the experiment. Only male mice were included in the study design due to potential effects of sex hormones. All experiments with animals were performed following protocols approved by the Animal Care and Use Committee of Jinzhou Medical University in accordance with the Care and Use of Laboratory Animals guidelines from the National Institutes of Health. All mice were randomized for stroke studies and treatments.

The MCAO model of acute ischemic stroke was prepared as previously reported [23-25]. Briefly, anesthesia was induced with 2% isoflurane in N₂O:O₂ (70%:30%). The right common carotid artery and ipsilateral internal carotid artery were exposed, and focal cerebral ischemia was produced by MCAO with a surgical nylon monofilament. After 60 min, reperfusion was allowed by withdrawal of the filament. In the sham group, the mice underwent an identical procedure without inserting the nylon monofilament. Body temperature during surgery was regularly maintained at 37.0±0.5°C by a homeothermic heating pad. The mice displayed typical neurologic deficit of MCAO, circling to the non-ischemic side (left), were included in this study. A total of 28 mice were excluded in this study.

Experimental design

For the time course study, mice were assigned to five groups: (1) Sham, (2) MCAO (6 h sacrifice (sac)), (3) MCAO (12 h sac), (4) MCAO (24 h sac), (5) MCAO (72 h sac).

For the dose and outcome study, mice were assigned to seven groups: (1) Sham (72 h sac), (2) MCAO + PBS (72 h sac), (3) MCAO + rh-NMNAT1 (3μg/kg, 72 h sac), (4) MCAO + rh-NMNAT1 (10μg/kg, 72 h sac), (5) MCAO + rh-NMNAT1 (30μg/kg, 72 h sac), (6) MCAO + PBS (24 h sac), (7) MCAO + rh-NMNAT1 (30μg/kg, 24 h sac).

For the mechanism study, mice were assigned to six groups (24 h sac or 72 h sac): (1) Sham, (2) MCAO + PBS, (3) MCAO + rh-NMNAT1 (30μg/kg), (4) MCAO + NAD, (5) MCAO + Negative siRNA + rh-NMNAT1

(30µg/kg), (6) MCAO + SIRT1 siRNA + rh-NMNAT1 (30µg/kg).

Drug administration

Intranasal administration was performed as previously described [26, 27]. Mice were placed on their backs and three doses (3 µg/kg, 10 µg/kg, 30 µg/kg) of recombinant human NMNAT1 (rh-NMNAT1, Sino Biological) were given. A total 10 µl of rh-NMNAT1 dissolved in PBS was delivered 1 h post MCAO within 10 min. Mice were then further kept on their backs for an additional 5 min to allow for absorption of drug before being returned to their cage. NAD⁺ (Sigma-Aldrich) dissolved in PBS was administered intraperitoneally at a dosage of 100 mg/kg according to previous reports [28, 29].

Intracerebroventricular injection

Pre-designed small interfering RNA (siRNA) targeting SIRT1 (RiboBio, Guangzhou, China) were stereotactically injected into the lateral ventricle of mice. Mice were anesthetized with pentobarbital sodium and then fixed in a stereotaxic apparatus. 24 h before MCAO, 2 µl of SIRT1 siRNA (300 pmol/µl) or a non-targeting negative control siRNA was injected into the right lateral ventricle at the point of 0.6 mm posterior to bregma, 1.5 mm lateral to bregma, and 1.7 mm ventral to the brain surface at the rate of 0.3 µl/min and the needle was kept in the place for 10 min.

Evaluation of BBB permeability in ischemic mice by Evan's Blue leakage

Evan's Blue (EB, 2% wt/vol in PBS, Sigma) was intravenously administered via tail vein. After 1 h circulation, the mouse was transcardially perfused with saline. The brain was removed and then cut into five 1-mm-thick coronal slices. Brain slices were photographed to visualize EB leakage. Quantitative assessment of BBB disruption was achieved by measuring EB content in the ischemic hemispheric tissue as we previously reported [30]. In brief, ischemic hemispheric tissue was weighed and homogenized in 50% wt/vol trichloroacetic acid. The fluorescence intensity of the supernatant was measured on a microplate fluorescence reader. The EB content was calculated using a standard curve and expressed as ng per g of brain tissue.

Measurements of neurological deficits

Neurological deficits of mice were assessed according to neurological disability status scale (NDSS) reported by Rodriguez et al [31]. NDSS has 10 progressive steps beyond 0 (normal), extending to status 10 (death). Motor performance was determined by the RotaRod test. Mice were trained to remain on the rod for 1.5 min at 50 revolutions/min for 3 days prior to MCAO. These mice were placed on the rotating rod after MCAO and the latency to fall was measured. Neurological deficit measurements were performed in a blinded way.

Measurements of infarct volume

After the evaluation of neurological deficits, the mouse was transcardially perfused with saline, and the brain was quickly removed and sliced into 1.0-mm-thick coronal sections. The brain sections were incubated for 15 min in a solution of 0.5% 2, 3, 5-triphenyltetrazolium chloride (TTC) at 37°C, and then the brain sections were scanned into a computer. The digital images of stained sections were recorded and analyzed using ImageJ software.

Immunofluorescence

Frozen 20- μ m-thick brain sections were blocked by 5% normal goat serum for 1 h and then incubated with primary antibodies overnights. The primary antibodies were: NMNAT1 (1:300, Santa Cruz Biotechnology USA), occludin (1:200, Invitrogen), claudin-5 (1:200, Invitrogen), SIRT1 (1:500, Invitrogen), and CD31 (an endothelial cell marker, 1:100, Santa Cruz Biotechnology), followed by Alexa Fluor 488 or Cy3-conjugated secondary antibodies (1:4000, Invitrogen) for 2 h at room temperature. The sections were then counterstained with 4', 6-diamidino-2-phenylindole (DAPI) for nuclear labeling. Fluorescence images were obtained by Leica DMI 4000B microscope (Leica, Germany).

Isolation of cerebral microvessels from the brain after ischemia/reperfusion

To examine the impacts of NMNAT1 on cerebral microvessels, we extracted cerebral microvessels from brains of ischemic mice as previously reported [32, 33]. Briefly, at the end of reperfusion, the hemispheric cerebral tissue was minced and homogenized in ice-cold PBS. Then the homogenate was filtered through a 41 μ m nylon mesh. Cerebral microvessels retained on the mesh were then purified with Dextran T-500 and stored at -80 °C until further analysis.

NAD⁺/NADH Assay

The NAD⁺ and NADH levels were measured using the NAD⁺/NADH Assay Kit (BioVision), according to the manufacturer's instructions.

Western blot analysis

Antibodies used in this study were NMNAT1 (1:500, Santa Cruz Biotechnology), occludin (1:500, Invitrogen), claudin-5 (1:500, Invitrogen), SIRT1 (1:1000, Invitrogen), acetyl-NF- κ B p65 (1:1000, Cell Signaling Technology), acetyl-p53 (1:1000, Cell Signaling Technology), cleaved Caspase-3 (1:500, ABclonal), MMP-9 (1:500, Invitrogen), β -actin (1:4000, Sigma) and corresponding secondary antibodies (1:5000, Invitrogen). The membranes were incubated with the primary antibody overnight and secondary antibodies for 1 h. The Enhanced Chemiluminescence (ECL) kit (GE Healthcare, UK) was employed to detect the signals. Protein levels were quantified by densitometry and normalized to β -actin, an internal standard.

Statistical analysis

Statistical analyses were performed using GraphPad Prism version 7. Data reported are presented as mean±SD. Statistical differences were evaluated with Student's *t*-test between two groups or by one-way analysis of variance (ANOVA) followed by all pairwise multiple comparison procedures using Bonferroni post-hoc test. *P* < 0.05 was defined as statistically significant.

Results

NMNAT1 was increased in ischemic microvessels after MCAO

To assess the NMNAT1 levels in the peri-infarct area of mice after MCAO, Western blot was used to evaluate NMNAT1 protein levels at 6 h, 12 h, 24 h and 72 h after MCAO. The data showed that NMNAT1 levels were significantly increased in the ischemic cerebral cortex of mice and also in microvessels isolated from ischemic brain at 6 h, 12 h, 24 h and 72 h after MCAO and peaked at 24 h after MCAO (Fig. 1a-d). Immunofluorescence staining showed that NMNAT1 colocalized extensively with CD31-positive brain microvascular endothelium in the peri-infarct area at 24 h after MCAO (Fig. 1e, f), suggesting an important role of NMNAT1 in ischemia-induced BBB disruption.

Rh-NMNAT1 treatment reduced infarct volume and improved neurological deficits after ischemia

To determine the best dose of rh-NMNAT1 on infarct volume, three doses were used: low (3 µg/kg), medium (10 µg/kg) and high (30 µg/kg). The results of Western blot demonstrated that NMNAT1 levels were increased in the cerebral cortex of mice after intranasal administration of rh-NMNAT1 (Fig. 2a, b). TTC staining showed that medium dose (10 µg/kg) of rh-NMNAT1 and high dose (30 µg/kg) of rh-NMNAT1 significantly reduced infarct volume at 72 h after MCAO when compared with PBS group (Fig. 2c, d). In addition, no significant difference was found in the infarct percentage with the low dose rh-NMNAT1 (3 µg/kg) when compared with PBS group (Fig. 2c, d).

NDSS and RotaRod tests were used to assess the neurological outcome in mice after MCAO. The results showed that mice in the PBS group performed significantly worse after MCAO when compared with the sham group in both tests (Fig. 2e, f). Both medium and high doses of rh-NMNAT1 improved neurological outcome compared with the PBS group after MCAO (Fig. 2e, f), while the high dose group (30 µg/kg) showed better neurological outcome as compared to the medium dose group (10 µg/kg) in RotaRod test. It is worth noting that rh-NMNAT1 (30 µg/kg) treatment did not affect cerebral blood flow (Supplementary Fig. 1) and other physiological parameters (Supplementary Table 1) compared to PBS group. Hence, the dose 30 µg/kg of rh-NMNAT1 was used for the following experiments.

Rh-NMNAT1 reduced BBB permeability through preventing the loss of occludin and claudin-5 in ischemic microvessels

To determine the effect of NMNAT1 on BBB disruption *in vivo*, mice were subjected to 1 h MCAO plus 24 h or 72 h reperfusion. The BBB permeability was determined by measuring EB extravasation. We observed that ischemia/reperfusion significantly increased the amount of extravasated EB in PBS-treated

MCAO group, whereas rh-NMNAT1 significantly reduced extravasation of EB in the ipsilateral hemispheres at 24 h and 72 h after MCAO, compared to control group, respectively (Fig. 3a, b).

To further determine whether the loss of TJPs in ischemic microvessels could be regulated by NMNAT1, we assessed occludin and claudin-5 protein levels by using immunofluorescent staining and Western blot approaches. The fluorescence intensity of occludin and claudin-5 was low in the peri-infarct area after 1 h MCAO plus 24 h or 72 h reperfusion, while treatment of rh-NMNAT1 prevented the loss of them in the ischemic microvessels (Fig. 3c, d). Western blot results also showed that levels of occludin and claudin-5 were decreased in isolated microvessels after 1 h MCAO plus 24 h or 72 h reperfusion, whereas rh-NMNAT1 treatment rescued the loss of them when compared with PBS groups (Fig. 3e-g). These findings indicate that rh-NMNAT1 attenuates ischemia-induced BBB permeability through inhibiting TJPs degradation.

Rh-NMNAT1 administration regulated the NAD⁺/SIRT1 signaling pathway

To explore the molecular pathways underlying NMNAT1-induced protection in brain injury, NAD⁺/SIRT1 signaling pathway was examined. As shown in Fig. 4a-c, the ischemia-induced depletion of NAD⁺ level and decrease in the NAD⁺/NADH ratio were observed in ischemic microvessels at 24 h after MCAO. SIRT1 protein level was significantly decreased in ischemic microvessels at 24 h after MCAO by using Western blot and immunofluorescent staining (Fig. 4d-f). These abnormalities were reversed by rh-NMNAT1 treatment (Fig. 4). These results indicate rh-NMNAT1 regulates NAD⁺/SIRT1 signaling pathway in ischemic microvessels.

Rh-NMNAT1 activated NAD⁺/SIRT1 pathway, inhibited cell apoptosis, and decreased MMP-9.

To further explore the potential mechanism of SIRT1 activation-induced protection, we targeted NF- κ B and p53, two vital downstreams of SIRT1. Compared with PBS-treated MCAO group, rh-NMNAT1 treatment significantly decreased the levels of acetylated NF- κ B and acetylated p53 in ischemic microvessels at 24 h after MCAO (Fig. 5b-d). Furthermore, rh-NMNAT1 treatment suppressed the levels of cleaved Caspase-3 and MMP-9 in ischemic microvessels 24 h after MCAO (Fig. 5b-f). Administration of SIRT1 siRNA abolished the effects of rh-NMNAT1 treatment (Fig. 5).

Rh-NMNAT1 administration ameliorated MCAO-induced brain injury via the NAD⁺/SIRT1 pathway

To investigate the role of NAD⁺/SIRT1 pathway in rh-NMNAT1's effects, we administered NAD⁺ or SIRT1 siRNA and measured SIRT1, occludin and claudin-5 levels in ischemic microvessels at 24 h after MCAO. The data from the Western blot showed that the levels of SIRT1, occludin and claudin-5 increased significantly in NAD⁺ group as compared to PBS group. The level of SIRT1 was significantly decreased with SIRT1 siRNA, which blocked the effects of rh-NMNAT1 (Fig. 6a-d). These results suggest that rh-NMNAT1 prevents the loss of occludin and claudin-5 via NAD⁺/SIRT1 signaling pathway.

To further clarify the role of NAD⁺/SIRT1 signaling pathway in the effect of rh-NMNAT1 on ischemia-induced cerebral injury, infarct volume was evaluated. Administration of SIRT1 siRNA abolished the neuroprotective effects of rh-NMNAT1 treatment (Fig. 6e, f). Administration of NAD⁺ mimicked the effect of rh-NMNAT1 that reduced the infarct volume (Fig. 6e, f). These results suggest that the effects of rh-NMNAT1 on ischemia-induced cerebral injury relate to NAD⁺/SIRT1 signaling pathway.

Discussion

In the present study, we observed the new mechanism underlying NMNAT1 protection in the model of transient cerebral ischemia and reperfusion. NMNAT1 levels increased in the peri-infarct cortex and specifically in microvessels after cerebral ischemia in mice. Intranasal administration of rh-NMNAT1 ameliorated infarct volume and improved neurologic deficits in mice with ischemic stroke. Meanwhile, rh-NMNAT1 administration attenuated cerebral ischemia-induced BBB injury. The novelty and important finding of the study is as follows: the observed beneficial effects of rh-NMNAT1 are likely attributed to BBB integrity via NAD⁺/SIRT1 signaling pathway in brain microvascular endothelial cells.

In this study, we found ischemia-induced increase in NMNAT1 level in the ischemic brain microvascular endothelial cells. However, we found that overexpression of NMNAT1 by rh-NMNAT1 administration after stroke reduced infarct volume and neurologic deficits. It may be because ischemia led to severe damage of cerebral cortex, and the auto-protection of spontaneous NMNAT1 up-regulation could only attenuate rather than reverse the pathological changes of ischemic brain.

Very importantly, the present study shows rh-NMNAT1 administration attenuated ischemia-induced BBB disruption in a mouse model of ischemic stroke. Given the vital role of BBB permeability in determining stroke outcome [34-36], we assessed its integrity by analysing EB leakage. In line with the reduced neurological impairment in stroke mice receiving rh-NMNAT1, BBB disruption was decreased after rh-NMNAT1 administration compared with control mice. Cerebral microvascular endothelial cells represent important therapeutic targets for many neurological diseases. TJPs (occludin and claudin-5), key molecules sealing the gaps between adjacent endothelial cells, are important for the maintenance of BBB integrity [37, 38]. To investigate the molecular mechanisms by which NMNAT1 preserves BBB integrity after ischemia/reperfusion brain injury, we focused on claudin-5 and occludin, two major TJPs, and cell apoptosis. The results show that rh-NMNAT1 rescued the loss of TJPs (occluding and claudin-5) and reduced apoptosis of constituent cells of cerebral microvessels during cerebral ischemia.

MMP-9 has been shown to regulate the degradation of TJPs [6, 38]. The involvement of MMP-9 in BBB disruption has been reported in several ischemic injury studies [39, 40]. Given this premise, we speculated that the MMP-mediated degradation of TJPs may be involved in the mechanism of NMNAT1-mediated BBB integrity after cerebral ischemia. Here, our results show that MMP-9 was induced in ischemic cerebral microvessels, and the change was accompanied by the loss of occludin and claudin-5. Rh-NMNAT1 was found to greatly decrease the level of MMP-9. These findings suggest that the MMPs-TJPs degradation pathway participates in NMNAT1-mediated BBB permeability during ischemia.

NAD⁺ has a critical role in energy metabolism and cell survival during cerebral ischemia [41]. As a NAD⁺-dependent deacetylase, SIRT1 deacetylates its downstreams, including p53 and NF-κB, to regulate cell apoptosis and inflammation under ischemia/hypoxia conditions [42, 43]. Inhibition of SIRT1 contributes to BBB disruption and aggravates brain edema in experimental subarachnoid hemorrhage [44]. Here, our results show that ischemia-induced depletion of NAD⁺ level and decrease in the NAD⁺/NADH ratio were associated with reduced SIRT1 level. Treatment with rh-NMNAT1 increased NAD⁺ availability and SIRT1 level. Our results also show that treatment of rh-NMNAT1 decreased the levels of acetylated p53 and acetylated NF-κB in MCAO mice, and SIRT1 siRNA blocked the effects of rh-NMNAT1. Finally, we found that NAD⁺ treatment rescued the loss of TJPs and reduced infarct volume after cerebral ischemia. The beneficial effects of rh-NMNAT1 treatment were blocked by SIRT1 siRNA. Overall, these findings demonstrate that rh-NMNAT1 could protect against ischemia-induced BBB injury after ischemic stroke, in part via regulation of NAD⁺/SIRT1 signaling pathway.

Conclusions

In conclusion, our findings demonstrate that administration of exogenous rh-NMNAT1 could attenuate infarct volume and improve neurological outcome. And rh-NMNAT1 could regulate ischemia-induced BBB permeability through NAD⁺/SIRT1 signaling pathway. Our results provide new insights into the mechanisms of BBB disruption after cerebral ischemia and suggest NMNAT1 is a regulator of BBB function that may be a potential therapeutic target for ischemic stroke.

Declarations

Acknowledgements Not applicable.

Authors' contribution Yang Zhang and Xun Guo performed the experiments and subsequent data analysis. Zhifeng Peng, Chang Liu and Lili Ren helped perform experiments and review the manuscript. Jia Liang and Peng Wang designed the study and prepared the manuscript. All authors read and approved the final manuscript.

Funding This study was supported by the National Natural Science Foundation of China (No. 81971231), the Scientific Research Project from the Educational Department of Liaoning Province (No. JYTQN2020011) and the Natural Science Foundation of Liaoning Province (No. 201602319).

Data Availability All data generated during this study are available from the corresponding author on reasonable request.

Code Availability Not applicable.

Ethics declarations

Ethics Approval All experiments with animals were performed following protocols approved by the Animal Care and Use Committee of Jinzhou Medical University in accordance with the Care and Use of Laboratory Animals guidelines from the National Institutes of Health.

Consent to Participate Not applicable.

Consent for Publication Not applicable.

Competing Interests The authors declare no competing interests.

References

1. Shi Y, Zhang L, Pu H, Mao L, Hu X, Jiang X, Xu N, Stetler RA, Zhang F, Liu X: Rapid endothelial cytoskeletal reorganization enables early blood–brain barrier disruption and long-term ischaemic reperfusion brain injury. *Nature communications* 2016, 7:10523.
2. Sifat AE, Vaidya B, Abbruscato TJ: Blood-brain barrier protection as a therapeutic strategy for acute ischemic stroke. *AAPS journal* 2017, 19(4):957-972.
3. Li Y, Zhong W, Jiang Z, Tang X: New progress in the approaches for blood–brain barrier protection in acute ischemic stroke. *Brain research bulletin* 2019, 144:46-57.
4. Rosell A, Ortega-Aznar A, Alvarez-Sabín J, Fernández-Cadenas I, Montaner J: Increased brain expression of matrix metalloproteinase-9 after ischemic and hemorrhagic human stroke. *Stroke* 2006, 37(6):1399-406.
5. Yang Y, Rosenberg GA: MMP-mediated disruption of claudin-5 in the blood-brain barrier of rat brain after cerebral ischemia. *Methods in molecular biology* 2011, 762:333-345.
6. Rosenberg GA, Yang Y: Vasogenic edema due to tight junction disruption by matrix metalloproteinases in cerebral ischemia. *Neurosurg focus* 2007, 22(5):E4.
7. Simard JM, Kent TA, Chen M, Tarasov KV, Gerzanich V: Brain oedema in focal ischemia: molecular pathophysiology and theoretical implications. *Lancet neurology* 2007, 6: 258–268.
8. Zhai RG, Rizzi M, Garavaglia S: Nicotinamide/nicotinic acid mononucleotide adenylyltransferase, new insights into an ancient enzyme. *Cellular & molecular life sciences* 2009, 66(17):2805-2818.
9. Shi X, Jiang Y, Kitano A, Hu T, Murdaugh RL, Li Y, Hoegenauer KA, Chen R, Takahashi K, Nakada D: Nuclear NAD⁺ homeostasis governed by NMNAT1 prevents apoptosis of acute myeloid leukemia stem cells. *Science advances* 2021, 7(30):eabf3895.
10. Yo S, Takashi N, Xianrong M, Aaron DA, Jeffrey M: NMNAT1 inhibits axon degeneration via blockade of SARM1-mediated NAD⁺ depletion. *ELife* 2016, 5:e19749.
11. Koenekoop RK, Wang H, Majewski J, Wang X, Lopez I, Ren H, Chen Y, Li Y, Fishman GA, Genead M, Schwartzentruber J, Solanki N, Traboulsi EI, Cheng J, Logan CV, McKibbin M, Hayward BE, Parry DA, Johnson CA, Nageeb M, Finding of Rare Disease Genes (FORGE) Canada Consortium, Poulter JA, Mohamed MD, Jafri H, Rashid Y, Taylor GR, Keser V, Mardon G, Xu H, Inglehearn CF, Fu Q, Toomes C,

- Chen R. Mutations in NMNAT1 cause Leber congenital amaurosis and identify a new disease pathway for retinal degeneration. *Nature genetics* 2012, 44(9):1035-1039.
12. Sasaki Y, Kakita H, Kubota S, Sene A, Lee TJ, Ban N, Dong Z, Lin JB, Boye SL, DiAntonio A, Boye SE, Apte RS, Milbrandt J. SARM1 depletion rescues NMNAT1-dependent photoreceptor cell death and retinal degeneration. *Elife*. 2020, 9:e62027.
 13. Kuribayashi H, Baba Y, Iwagawa T, Arai E, Murakami A, Watanabe S. Roles of Nmnat1 in the survival of retinal progenitors through the regulation of pro-apoptotic gene expression via histone acetylation. *Cell death & disease* 2018, 9(9):891.
 14. Jiang H, Wan Z, Ding Y, Yao Z: Nmnat1 modulates mitochondrial oxidative stress by inhibiting caspase-3 signaling in Alzheimer's disease. *Journal of molecular neuroscience* 2021, (7):1467-1472.
 15. Garten A, Schuster S, Penke M, Gorski T, de Giorgis T, Kiess W: Physiological and pathophysiological roles of NAMPT and NAD metabolism. *Nature reviews endocrinology* 2015, 11(9):535-546.
 16. Zhang DX, Zhang JP, Hu JY, Huang YS: The potential regulatory roles of NAD(+) and its metabolism in autophagy. *Metabolism* 2016, 65(4):454-462.
 17. Poltronieri P, Celetti A, Palazzo L: Mono(ADP-ribosyl)ation enzymes and NAD⁺ metabolism: a focus on diseases and therapeutic perspectives. *Cells* 2021,10(1):128.
 18. Zhou CC, Yang X, Hua X, Liu J, Fan MB, Li GQ, Song J, Xu TY, Li ZY, Guan YF, Wang P, Miao CY: Hepatic NAD(+) deficiency as a therapeutic target for non-alcoholic fatty liver disease in ageing. *British journal of pharmacology* 2016, 173(15):2352-2368.
 19. Hu Q, Manaenko A, Bian H, Guo Z, Huang JL, Guo ZN, Yang P, Tang J, Zhang JH: Hyperbaric oxygen reduces infarction volume and hemorrhagic transformation through ATP/NAD(+)/Sirt1 pathway in hyperglycemic middle cerebral artery occlusion rats. *Stroke* 2017, 48(6):1655-1664.
 20. Wang P, Xu TY, Guan YF, Tian WW, Viollet B, Rui YC, Zhai QW, Su DF, Miao CY: Nicotinamide phosphoribosyltransferase protects against ischemic stroke through SIRT1-dependent adenosine monophosphate-activated kinase pathway. *Annals of neurology* 2011, 69(2):360-374.
 21. Liang J, Wang P, Wei J, Bao C, Han D: Nicotinamide mononucleotide adenylyltransferase 1 protects neural cells against ischemic injury in primary cultured neuronal cells and mouse brain with ischemic stroke through AMP-activated protein kinase activation. *Neurochemical research* 2015, 40(6):1102-1110.
 22. Wang P, Lu Y, Han D, Wang P, Ren L, Bi J, Liang J: Neuroprotection by nicotinamide mononucleotide adenylyltransferase 1 with involvement of autophagy in an aged rat model of transient cerebral ischemia and reperfusion. *Brain research* 2019, 1723:146391.
 23. Wang P, Liang J, Li Y, Li J, Yang X, Zhang X, Han S, Li S, Li J: Down-regulation of miRNA-30a alleviates cerebral ischemic injury through enhancing beclin 1-mediated autophagy. *Neurochemical research* 2014, 39(7):1279-1291.
 24. Wang P, Zhang N, Liang J, Li J, Han S, Li J: Micro-RNA-30a regulates ischemia-induced cell death by targeting heat shock protein HSPA5 in primary cultured cortical neurons and mouse brain after stroke. *Journal of neuroscience research* 2015, 93(11):1756-1768.

25. Wang P, Liang X, Lu Y, Zhao X, Liang J: MicroRNA-93 Downregulation ameliorates cerebral ischemic injury through the Nrf2/HO-1 defense pathway. *Neurochemical research* 2016, 41(10):2627-2635.
26. Zhang Y, Chen Y, Wu J, Manaenko A, Yang P, Tang J, Fu W, Zhang JH: Activation of dopamine D2 receptor suppresses neuroinflammation through α B-crystalline by inhibition of NF- κ B nuclear translocation in experimental ICH mice model. *Stroke* 2015, 46(9):2637-2646.
27. Shi X, Xu L, Doycheva DM, Tang J, Yan M, Zhang JH: Sestrin2, as a negative feedback regulator of mTOR, provides neuroprotection by activation AMPK phosphorylation in neonatal hypoxic-ischemic encephalopathy in rat pups. *Journal of cerebral blood flow and metabolism* 2017, 37(4):1447-1460.
28. Zheng C, Han J, Xia W, Shi S, Liu J, Ying W: NAD(+) administration decreases ischemic brain damage partially by blocking autophagy in a mouse model of brain ischemia. *Neuroscience letters* 2012, 512(2):67-71.
29. Wang B, Ma Y, Kong X, Ding X, Gu H, Chu T, Ying W: NAD(+) administration decreases doxorubicin-induced liver damage of mice by enhancing antioxidation capacity and decreasing DNA damage. *Chemico-biological interactions* 2014, 212:65-71.
30. Liu W, Hendren J, Qin XJ, Shen J, Liu KJ: Normobaric hyperoxia attenuates early blood-brain barrier disruption by inhibiting MMP-9-mediated occludin degradation in focal cerebral ischemia. *Journal of neurochemistry* 2009, 108(3):811-820.
31. Rodriguez R, Santiago-Mejia J, Gomez C, San-Juan ER: A simplified procedure for the quantitative measurement of neurological deficits after forebrain ischemia in mice. *Journal of neuroscience methods* 2005, 147(1):22-28.
32. Wang P, Pan R, Weaver J, Jia M, Liu KJ: MicroRNA-30a regulates acute cerebral ischemia-induced blood-brain barrier damage through ZnT4/zinc pathway. *Journal of cerebral blood flow and metabolism* 2021, 41(3):641-655.
33. Liu W, Sood R, Chen Q, Sakoglu U, Hendren J, Çetin Ö, Miyake M, Liu KJ: Normobaric hyperoxia inhibits NADPH oxidase-mediated matrix metalloproteinase-9 induction in cerebral microvessels in experimental stroke. *Journal of neurochemistry* 2010, 107(5):1196-1205.
34. Obermeier B, Daneman R, Ransohoff RM. Development, maintenance and disruption of the blood-brain barrier. *Nature medicine* 2013, 19(12):1584-96.
35. Abdullahi W, Tripathi D, Ronaldson PT. Blood-brain barrier dysfunction in ischemic stroke: targeting tight junctions and transporters for vascular protection. *American journal of physiology-cell physiology* 2018, 315(3):C343-C356.
36. Jiang X, Andjelkovic AV, Zhu L, Yang T, Bennett MVL, Chen J, Keep RF, Shi Y: Blood-brain barrier dysfunction and recovery after ischemic stroke. *Progress in neurobiology* 2018, 163-164:144-171.
37. Wolburg H, Lippoldt A: Tight junctions of the blood-brain barrier: development, composition and regulation. *Vascular pharmacology* 2002, 38(6):323-337.
38. Jie L, Jin X, Ke JL, Liu W: Matrix metalloproteinase-2-mediated occludin degradation and caveolin-1-mediated claudin-5 redistribution contribute to blood-brain barrier damage in early ischemic stroke stage. *Journal of neuroscience* 2012, 32(9):3044.

39. Suofu Y, Clark JF, Broderick JP, Kurosawa Y, Wagner KR, Lu A: Matrix metalloproteinase-2 or -9 deletions protect against hemorrhagic transformation during early stage of cerebral ischemia and reperfusion. *Neuroscience* 2012, 212:180-189.
40. Sarkar S, Mukherjee A, Das N, Swarnakar S: Protective roles of nanomelatonin in cerebral ischemia-reperfusion of aged brain: Matrixmetalloproteinases as regulators. *Experimental gerontology* 2017, 92:13-22.
41. Huang Q, Sun M, Li M, Zhang D, Han F, Wu JC, Fukunaga K, Chen Z, Qin ZH: Combination of NAD(+) and NADPH offers greater neuroprotection in ischemic stroke models by relieving metabolic stress. *Molecular neurobiology* 2018, 55(7):6063-6075.
42. Meng X, Tan J, Li M, Song S, Zhang Q: Sirt1: role under the condition of ischemia/hypoxia. *Cellular & Molecular Neurobiology* 2016, 37(1):1-12.
43. Hernández-Jiménez M, Hurtado O, Cuartero MI, Ballesteros I, Moraga A, Pradillo JM, McBurney MW, Lizasoain I, Moro MA: Silent information regulator 1 protects the brain against cerebral ischemic damage. *Stroke* 2013, 44(8):2333-2337.
44. Zhou XM, Zhang X, Zhang XS, Zhuang Z, Li W, Sun Q, Li T, Wang CX, Zhu L, Shi JX, Zhou ML: SIRT1 inhibition by sirtinol aggravates brain edema after experimental subarachnoid hemorrhage. *Journal of neuroscience research* 2014, 92(6):714-722.

Figures

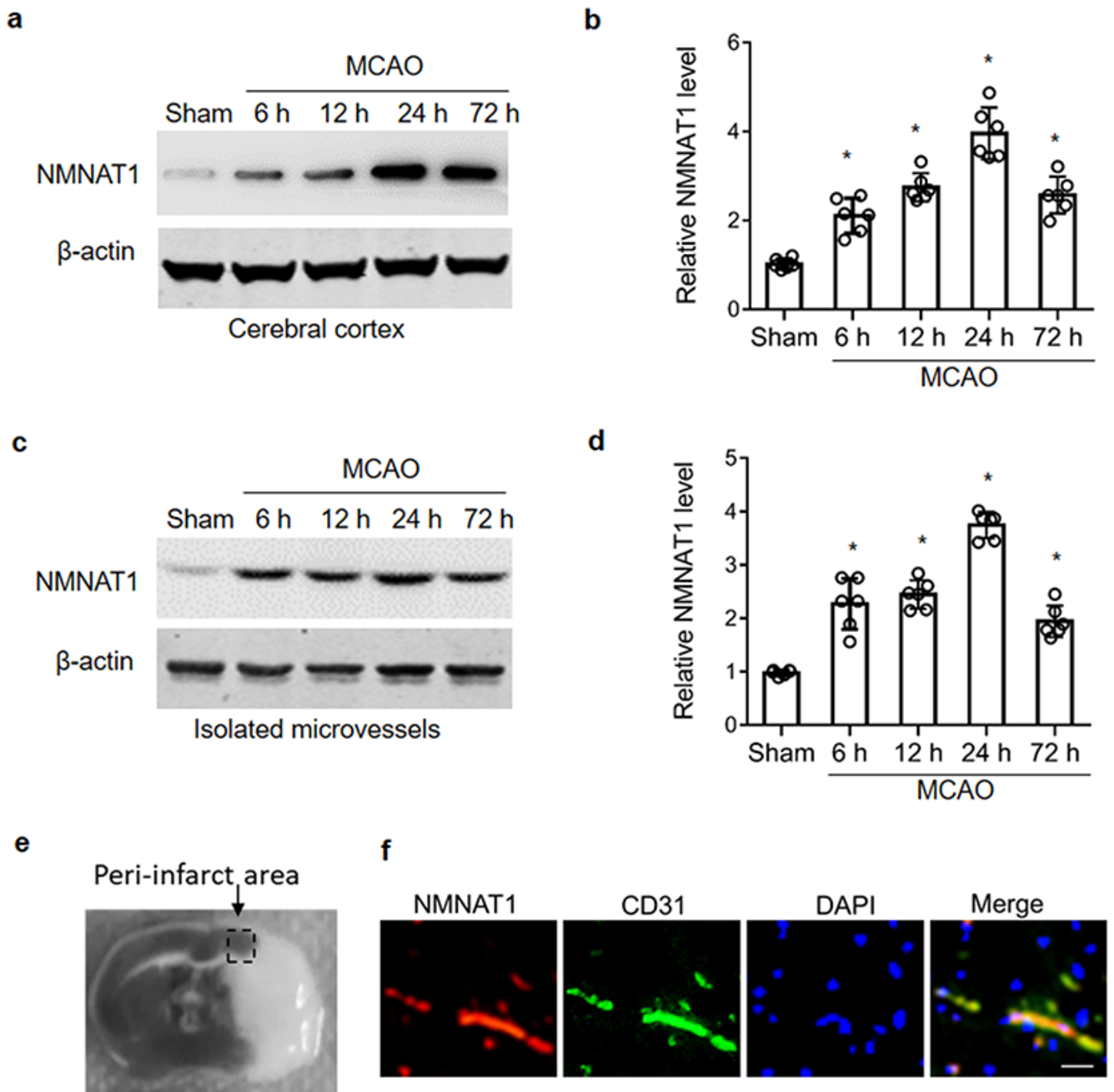


Figure 1

NMNAT1 levels in the brain of mice with ischemic stroke. (a) Typical results of Western blot showed NMNAT1 protein levels in the cerebral cortex of mice. (b) The quantitative analysis demonstrated that NMNAT1 levels were up-regulated in the cerebral cortex of mice at 6 h, 12 h, 24 h and 72 h after MCAO. (c) Typical results of Western blot showed NMNAT1 protein levels in microvessels isolated from ischemic mice. (d) The quantitative analysis demonstrated that NMNAT1 levels were up-regulated in microvessels isolated from ischemic mice at 6 h, 12 h, 24 h and 72 h after MCAO. (e) Representative image of the peri-

infarct cortex. (f) Representative images of immunofluorescent staining for NMNAT1 in neurons and brain microvascular endothelial cells of brain slices. Images were acquired from the peri-infarct cortex. Scale bar, 20 μ m. * P <0.05 versus Sham. Data are expressed as mean \pm SD (n=6 per group).

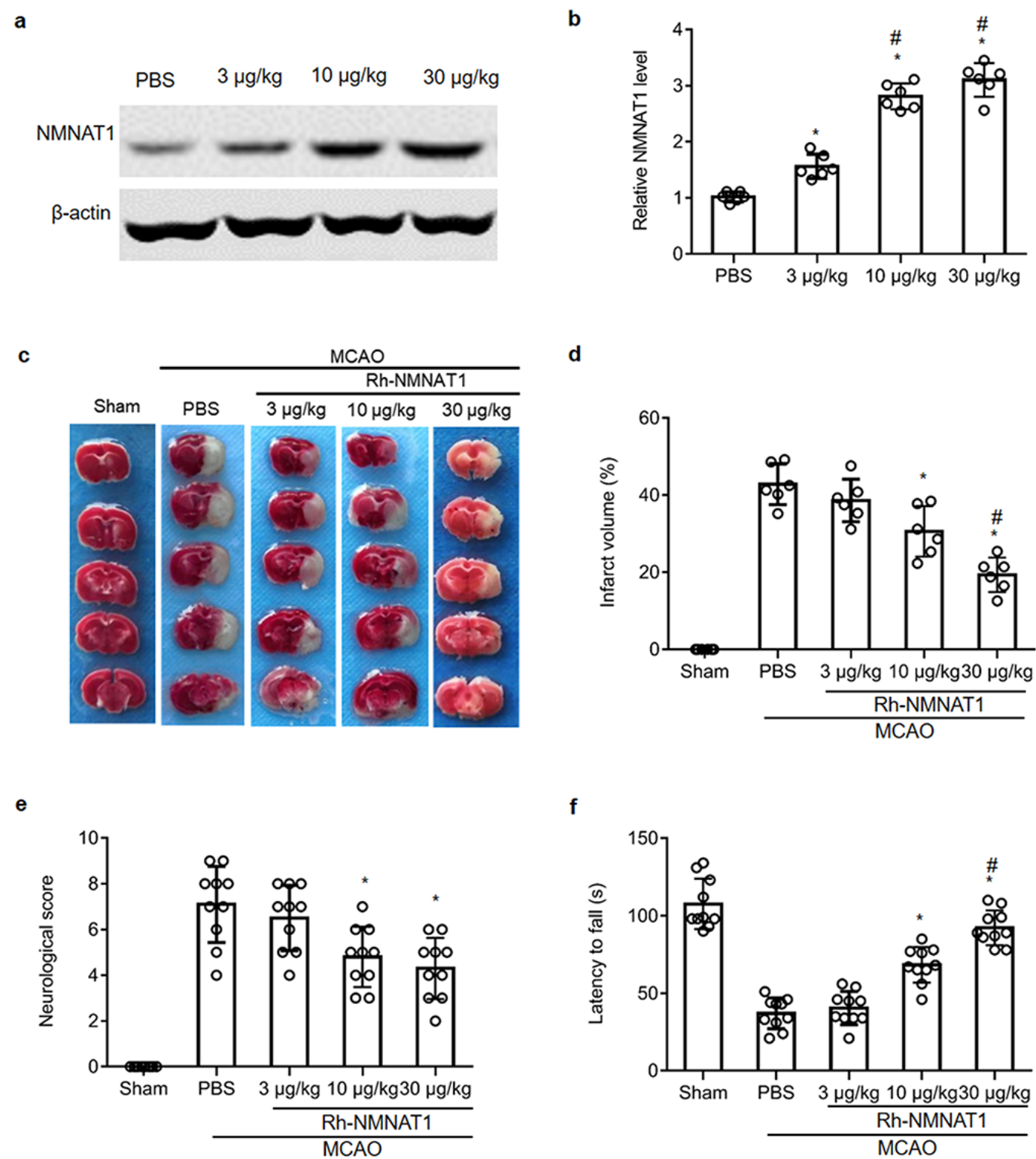


Figure 2

Effects of intranasal administration of rh-NMNAT1 on brain infarction and neurological function. (a) Typical results of Western blot showed NMNAT1 protein levels in the cerebral cortex of mice. (b) The

quantitative analysis demonstrated that NMNAT1 levels were up-regulated in the cerebral cortex of mice after intranasal administration of rh-NMNAT1. * $P < 0.05$ vs. PBS group, # $P < 0.05$ vs. Rh-NMNAT1 (3 μ g/kg)-treated group. Data are expressed as mean \pm SD (n=6 per group). (c) Typical images of TTC staining illustrating infarction in mice with 1 h MCAO plus 72 h reperfusion. (d) Quantitative analysis of infarct volumes. Data are expressed as mean \pm SD (n=6 per group). (e) and (f) Neurological deficits were assessed using the NDSS test (e) and the RotaRod test (f). * $P < 0.05$ vs. PBS-treated MCAO group, # $P < 0.05$ vs. Rh-NMNAT1 (10 μ g/kg)-treated MCAO group. Data are expressed as mean \pm SD (n=10 per group).

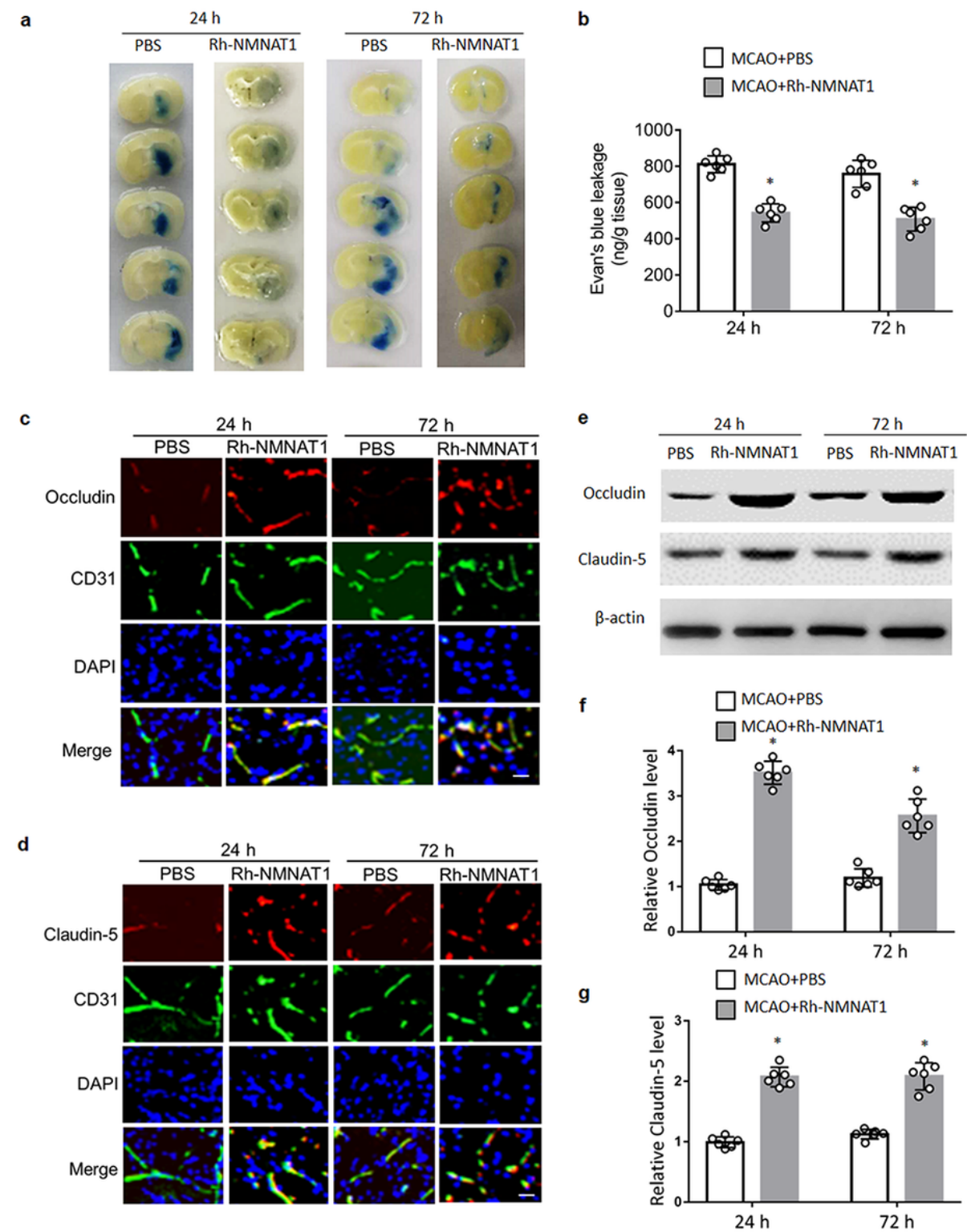


Figure 3

Effects of rh-NMNAT1 on BBB permeability in ischemic mice. (a) EB extravasation was measured to evaluate the BBB permeability at 24 h and 72 h after MCAO. Brain slices showed EB extravasation (blue dye leakage). (b) Quantitative analysis showed EB content in ischemic hemisphere. (c) Co-staining of occludin (red), CD31 (green) and DAPI (blue) in the peri-infarct cortex. (d) Co-staining of claudin-5 (red), CD31 (green) and DAPI (blue) in the peri-infarct cortex. Scale bar: 20 μ m. (e) Representative bands of occludin and claudin-5 in microvessels isolated from ischemic mice using Western blot. (f) Quantitative analysis of occludin. (g) Quantitative analysis of claudin-5. *P < 0.05 vs. PBS-treated MCAO group. Data are expressed as mean \pm SD (n=6 per group).

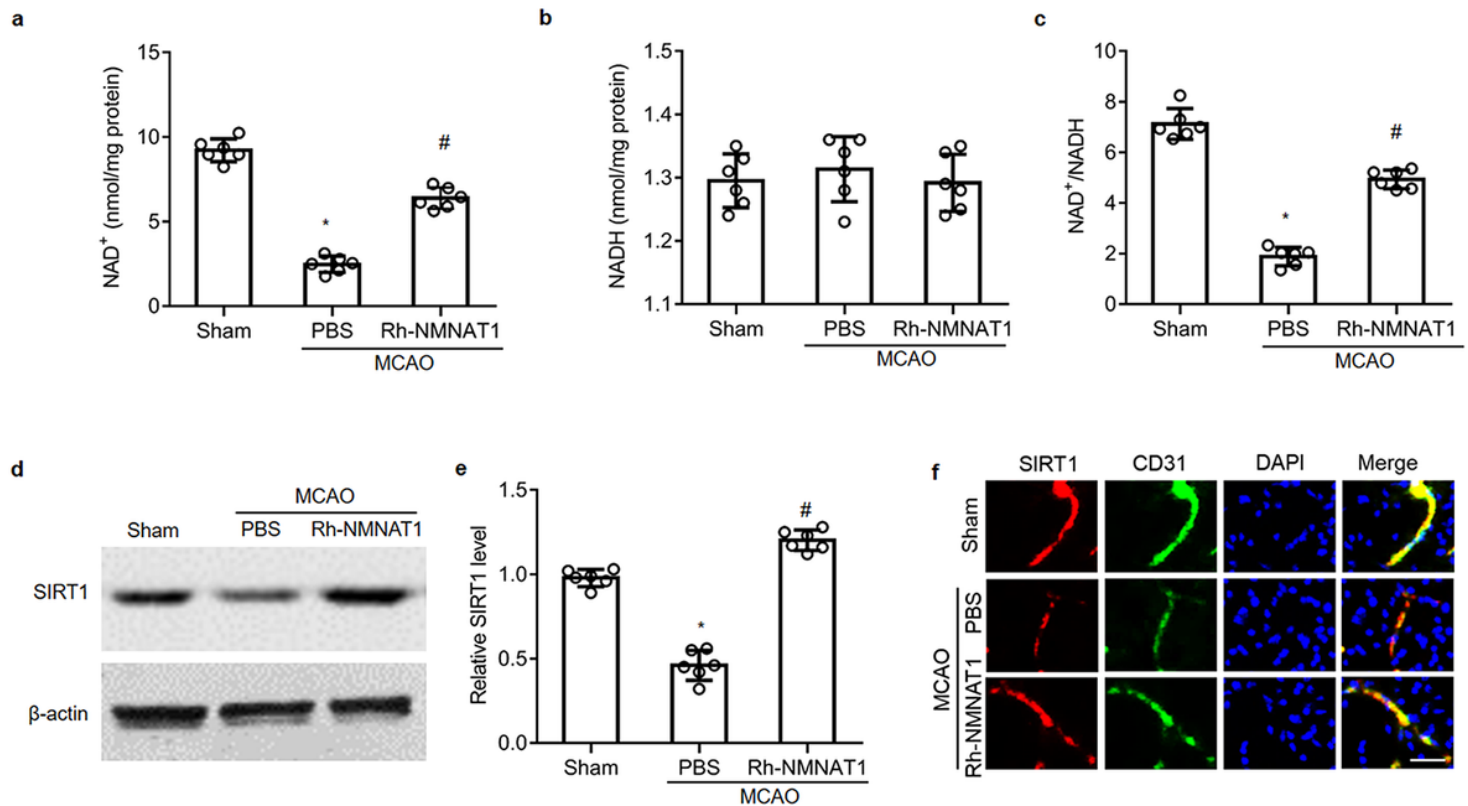


Figure 4

The effects of rh-NMNAT1 on the NAD⁺/SIRT1 signaling pathway. (a) NAD⁺ level in ischemic microvessels at 24 h after MCAO. (b) NADH level in ischemic microvessels at 24 h after MCAO. (c) NAD⁺/NADH ratio in ischemic microvessels at 24 h after MCAO. (d) Representative bands of SIRT1 in microvessels isolated from ischemic mice using Western blot. (e) Quantitative analysis of SIRT1. (f) Co-staining of SIRT1 (red), CD31 (green) and DAPI (blue) in the peri-infarct cortex. Scale bar: 20 μ m. *P < 0.05 vs. Sham, #P < 0.05 vs. PBS-treated MCAO group. Data are expressed as mean \pm SD (n=6 per group).

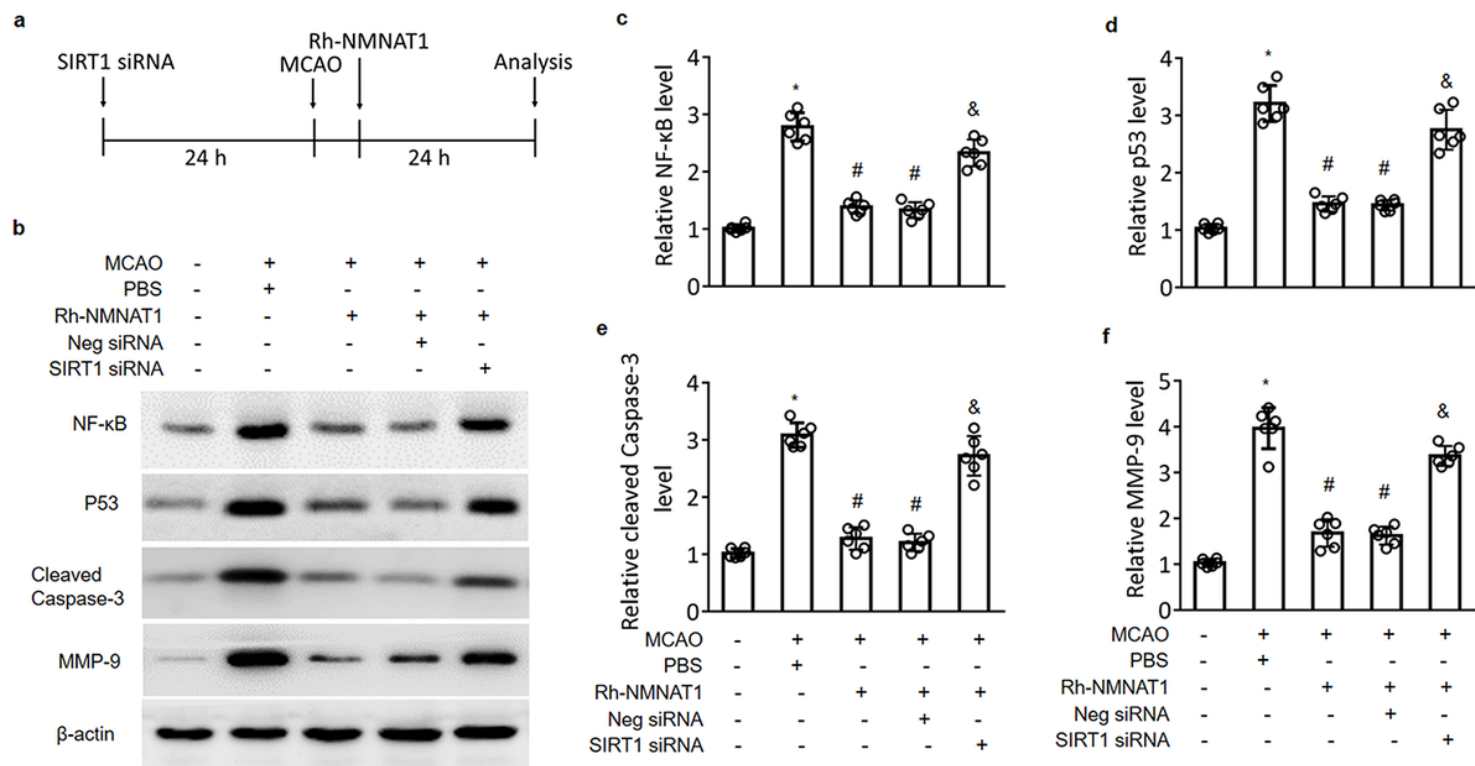


Figure 5

Rh-NMNAT1 induced activation of NAD⁺/SIRT1 pathway, decreased apoptosis, and inhibited MMP-9. (a) Schematic diagram of the experimental design. (b) Representative picture of Western blot showing bands of the levels of acetylated NF-κB, acetylated p53, cleaved Caspase-3 and MMP-9 in ischemic microvessels at 24 h after MCAO. (c) Quantitative analysis of acetylated NF-κB. (d) Quantitative analysis of acetylated p53. (e) Quantitative analysis of cleaved Caspase-3. (f) Quantitative analysis of MMP-9. *P<0.05 vs. Sham, #P <0.05 vs. PBS-treated MCAO group, &P<0.05 vs. Rh-NMNAT1+Neg siRNA. Data are expressed as mean±SD (n=6 per group). Neg siRNA: negative control siRNA.

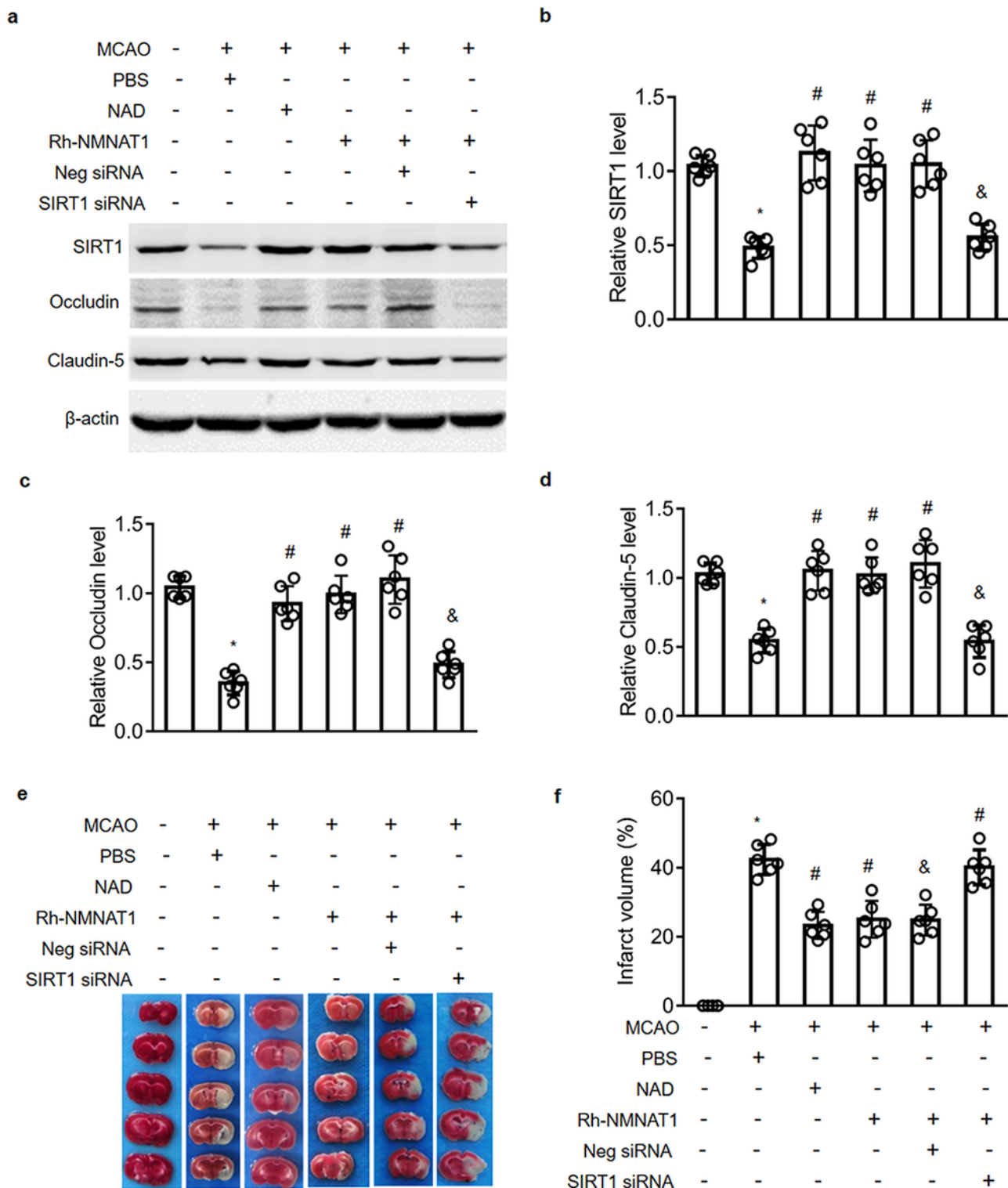


Figure 6

Effect of NAD⁺, rh-NMNAT1 and SIRT1 siRNA on brain injury. (a) Representative picture of Western blot data showing bands of the levels of SIRT1, occludin and claudin-5 in microvessels isolated from ischemic mice with 1 h MCAO plus 24 h reperfusion. (b) Quantitative analysis of SIRT1. (c) Quantitative analysis of occludin. (d) Quantitative analysis of claudin-5. (e) Typical images of TTC staining illustrating infarction in mice with 1 h MCAO plus 72 h reperfusion. (f) Quantitative analysis of infarct volumes.

*P<0.05 vs. Sham, #P <0.05 vs. PBS-treated MCAO group, &P<0.05 vs. Rh-NMNAT1+Neg siRNA. Data are expressed as mean±SD (n=6 per group). Neg siRNA: negative control siRNA.

Supplementary Files

This is a list of supplementary files associated with this preprint. Click to download.

- [Supplementaryinformation.pdf](#)